

Cellular responses to novel, micropatterned biomaterials*

Marga C. Lensen[‡], Vera A. Schulte, Jochen Salber, Mar Diez, Fabian Menges, and Martin Möller

DWI e.V. and Institute of Technical and Macromolecular Chemistry, RWTH Aachen, Pauwelsstrasse 8, D-52056 Aachen, Germany

Abstract: Two UV-curable polymers, i.e., a star-shaped poly(ethylene glycol) (PEG) and a linear perfluorinated polyether (PFPE), are investigated as novel biomaterials in a systematic study of the cellular responses to surface chemistry, topography, and elasticity. Based on the wettability it was expected that the two novel biomaterials were too hydrophilic or -phobic, respectively, to support cell adhesion. Indeed, no cell adhesion was observed on the smooth, unstructured elastomers, whereas the materials showed no cytotoxicity. However, when the materials bear defined, topographic patterns (prepared by UV-based imprinting), cells do react strongly to the surfaces; they adhere, spread, and change their shape depending on the geometry of the features. Typically, cells were found to align along line patterns and “float” on pillar structures. It should be noted that the chemistry of the surface is not altered by the imprinting process, hence, there are no biofunctional molecules present at the surface to aid the cell adhesion. Finally, a remarkable effect of elasticity on the cellular behavior was discovered. Thus, the three parameters of chemistry, topography, and elasticity were investigated in- and interdependently, and it was found that the biomaterials may lose their resistance to protein adsorption and cell adhesion depending on the surface topography.

Keywords: biomaterials; patterning; cells; wettability; hydrogel.

INTRODUCTION

Over the last decades, a vast amount of research has been dedicated to the development of novel materials for biomedical applications such as tissue engineering, proteomics, prosthetics, and regenerative medicine. Correspondingly, much is known about the processes that take place when biomaterials are brought into contact with biological fluids (e.g., blood, urine, or saliva). It is established that upon the first contact, proteins from the medium adsorb to the foreign interface [1]. This initial process of protein adsorption may be very unspecific, however, it determines the follow-up events such as cell adhesion and (in)growth [2]. The spontaneous adsorption processes are not always desired (e.g., protein adsorption on contact lenses or cell growth on implants) since they can lead to unwanted cascade reactions, such as inflammation [3]. Furthermore, in the development of biosensors, selectivity and sensitivity are severely hampered by unspecific protein adsorption. Therefore, a lot of research has focused on the development of inert, protein-resistant materials and coatings [4]. Only when the nonspecific

*Paper based on a presentation at the 3rd International Symposium on Novel Materials and Their Synthesis (NMS-III) and the 17th International Symposium on Fine Chemistry and Functional Polymers (FCFP-XVII), 17–21 October 2007, Shanghai, China. Other presentations are published in this issue, pp. 2231–2563.

[‡]Corresponding author

protein adsorption and cell adhesion are effectively suppressed, one can introduce binding sites for specific biointeraction in a controlled way.

Protein adsorption and cell adhesion to surfaces depend on a variety of interdependent factors of which the chemical, physical, and mechanical properties of the surface are most accessible to investigate systematically. Thus, numerous studies have been carried out in which the chemical properties (e.g., hydrophobicity) were systematically varied, and a certain optimal wettability has been discovered [5,6]. At the same time, many researchers have dedicated their efforts to elucidate the effect of topography, i.e., the micro- or nanosized surface structure on cell adhesion [7–13]. For instance, cells were observed to align and elongate on micrometer grooved surfaces, an effect denoted “contact guidance” [14–18]. Finally, recent studies have revealed that cells “sense” the substrate’s stiffness and tend to prefer stiffer substrates onto which they can exert traction forces upon adhesion and migration [19–25]. It should be noted that the choice of cell type is also important, since different cell types may respond very differently to similar surfaces.

Although a lot of research has been undertaken to study systematically the effects of chemistry, topography, and elasticity of the surface [26–30], similar investigations, for instance, concerning cellular responses on topographic patterns, too often yield contradictory results. The reason for this could be that the three aforementioned parameters cannot be considered independently; a topographically structured surface may not have the same wettability as a smooth surface of the same material. Besides, each material with a defined surface chemistry still has a certain inherent roughness (i.e., nanotopography) to which cells may respond. At last, results obtained from cell studies on defined topographic patterns on hard (e.g., metallic) surfaces cannot be extrapolated to soft materials (e.g., elastomers or gels) even if the surface chemistry is comparable. It is, therefore, of great interest to take the three interdependent effects (i.e., chemistry, topography, and elasticity) into consideration simultaneously, and the first results are presented here.

EXPERIMENTAL PROCEDURES

Synthesis and materials

All chemicals were purchased from Aldrich and used as received, unless stated otherwise. Solvents were at least analytical-grade quality. The silicon masters used in these studies were purchased from Amo GmbH (Aachen).

The synthesis of the acrylate-functionalized star poly(ethylene glycol) (PEG) was performed according to the following procedure [31]. Prior to the end-capping reaction, the hydroxyl-terminated star PEG (Dow Chemical) was precipitated in cold diethyl ether ($-80\text{ }^{\circ}\text{C}$) and dried thoroughly during 4 h at 10^{-2} mbar at $80\text{ }^{\circ}\text{C}$ oil bath temperature. Under a nitrogen atmosphere, 0.4 g (1.3 equiv) of acrylic anhydride was slowly added to a mixture of 5.0 g of the star PEG prepolymer and 0.3 ml (1.5 equiv) of water-free pyridine in 15 ml of toluene. The resulting mixture was stirred for 24 h at room temperature. After removal of the solvent and pyridine, the crude product was dried at room temperature during 8 h at 10^{-2} mbar. Unreacted acrylic anhydride was separated from the product by precipitation in diethyl ether at $-80\text{ }^{\circ}\text{C}$ (stirring at maximum speed), leaving the product as a colorless oil. The purified product was dried at room temperature during 8 h at 10^{-3} mbar. The purity of the product was verified by matrix-assisted laser desorption ionization–time-of-flight (MALDI–TOF), ^1H -NMR, and ^{13}C -NMR (600 MHz), and gel permeation chromatography (GPC) (tetrahydrofuran, THF). The results confirmed that all six end-groups were acrylated.

The functionalization of perfluorinated polyether (PFPE) diol (Solvay Solexis; $M_n \sim 1900\text{ g/mol}$) with acrylate end-groups was performed according to a procedure adopted from literature and described [31]. Typically, 0.86 ml (6 mmol) of 2-isocyanatoethyl methacrylate and 50 ml of dibutyltin diacetate (DBTDA) as a catalyst were added to a solution of 5.7 g (3 mmol) of PFPE diol in 2 ml of 1,1,2-trifluor-1,2,2-trichloroethane (Freon 113). The reaction mixture was stirred during 24 h at $50\text{ }^{\circ}\text{C}$, after which

the solvent was removed. The crude product was purified by multiple precipitations in petrol ether or hexane. The purity of the product, PFPE dimethyl acetamide (DMA) was verified by NMR.

UV-curing

UV-based imprinting was performed as follows [31]. Typically, 1 g of PFPE DMA was dissolved in 0.5 ml of Freon together with 10 mg (1 wt %) of the photoinitiator benzoin methyl ether. After homogenization, the solvent was evaporated under a mild stream of nitrogen. The viscous prepolymer mixture was drop-cast on a master substrate in a nitrogen-filled glovebox, where the UV-curing was carried out under a UV-lamp ($\lambda = 366$ nm) positioned about 8 cm above the sample. After curing, the elastomeric replica was mechanically peeled off (with tweezers). The UV-based imprinting of acrylate star PEG was carried out in analogy to the procedure described for PFPE DMA. In this case, acetone was used as a solvent for the star PEG precursor. Typically, 200 μ l of the star PEG was mixed with an acetone solution of the photoinitiator benzoin methyl ether (1 wt %) and pentaerythritol triacrylate (PETA) as a cross-linking agent (5 wt %). For PEG material with variable elasticities, various concentrations of photoinitiator (0.5–1.5 wt %) and cross-linker (0–15 wt %) were used. After thorough mixing and subsequent evaporation of the solvent, the photocurable mixture was drop-cast on a patterned master. The UV-curing was carried out under ambient conditions until complete polymerization. The replica was peeled off mechanically (with tweezers).

Contact angle measurements

Static water contact angle measurements were carried out according to the sessile drop technique except for the PEG material, using a Krüss G2 goniometer. Droplets (5 μ l) of deionized water were placed on the surface-air side of the samples at ambient conditions. On every sample, at least eight measurements were performed and the values were averaged. The contact angle of the PEG material was derived from captive bubble measurements, using a Krüss G-23 goniometer microscope. To static contact angle of the air bubble at the interface of PEG with water was determined by taking the average value of the visually observed left and right contact angles. Six measurements were carried out during 3 h at different spots on the sample, and the goniometrically determined values were averaged. Advancing and receding contact angles were measured by the Wilhelmy plate method. Rectangular sample slides ($\sim 1 \times 2$ cm²) were dipped 6 mm deep in deionized water at room temperature. On every sample, at least three measurements were performed.

Surface energy

The surface free energy was detected by sessile drop method on Krüss G2 goniometer. At least two of three solutions (ethylene glycol, diiodmethane, deionized water) were used. For analysis, the method after Owens-Wendt-Rabel and Kaelble was selected. All chemicals were purchased from Aldrich and used as received, unless stated otherwise. Solvents were at least analytical-grade quality. The silicon masters used in these studies were purchased from Amo GmbH (Aachen).

Cell studies

Mouse fibroblast cell line NIH L929 was used. Cells were cultured in culture flasks at 37 °C in a 5 % CO₂ supplied incubator. The culture media was RPMI-1460 (PAA) supplemented with 10 % fetal bovine serum (PAA) and 1 % penicillin/streptomycin (PAA). The culture medium was changed every two days. Cells were harvested with 0.25 % trypsin (PAA), and suspensions of 50 000–100 000 cells/ml were prepared with RPMI medium. Substrates were placed in microwell plates, rinsed three

times with sterile water and phosphate buffered saline (PBS) (PAA), respectively before adding the cell solution.

Cell adhesion and spreading was monitored at different cultivation times (1 h to 5 d) by light microscopy on an Axiovert 100A Imaging microscope (Carl Zeiss AG), an optical reflection microscope equipped with a differential interference contrast (DIC) module. Pictures were taken using an AxioCam MRc digital camera and analyzed using the AxioVison 40 V4.6.1.0 software package (Carl Zeiss AG). Viability staining (Live/Dead Staining kit, Invitrogen) and F-Actin staining with AlexaFluor 568 phalloidin (Mol. Probes) were carried out according to protocol.

For the scanning electron microscopy studies, the cells were rinsed three times with PBS and fixed with 2 % paraformaldehyde for at least 1 h, followed by dehydration through an ethanol series. Specimens were observed by a field emission scanning electron microscope (S-4800, Hitachi) using an accelerating voltage of 1.0 kV and a working distance of 8 mm.

RESULTS AND DISCUSSION

In order to elucidate the roles of different parameters separately and in combination, we use materials which chemical, topographic, and mechanical properties can be tuned. We have chosen UV-curable prepolymers with desired chemical properties to form surfaces that are either smooth or that bear a defined topography and which mechanical properties can be tuned by varying the cross-linking density [25,30,32].

Cell adhesion as a function of wettability

Chemical properties of the biomaterials

From several systematic studies of the dependence of cell adhesion on the wettability of the substrate consensus, an optimum in cell adhesion vs. wettability has been reached; cells (e.g., fibroblasts) do not like to adhere on too hydrophilic or -phobic surfaces. Not surprisingly, tissue culture polystyrene (TCPS) has an optimum, intermediate wettability while hydrogels (e.g. PEG) are very hydrophilic and known for their cell-repellent properties [4,33–35]. Figure 1 depicts the relation between cell adhesion and surface chemistry (based on literature reports) [6], showing that the maximal adherence of cells (fibroblasts) occurs on surfaces with an intermediate wettability, i.e., with a water contact angle of roughly between 55 and 85°.

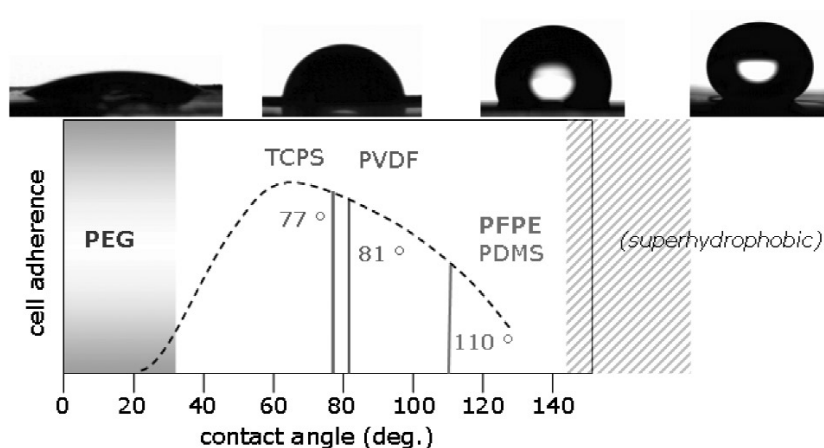
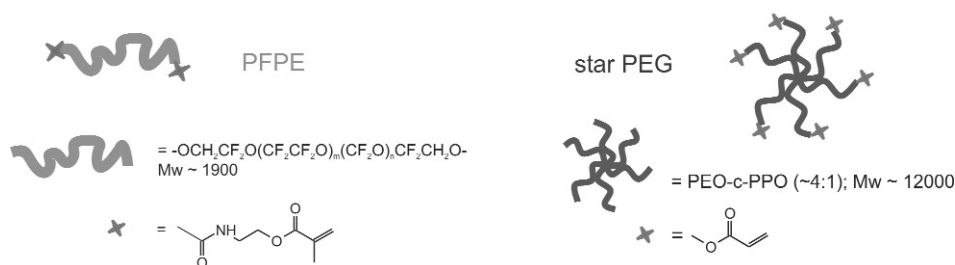


Fig. 1 Sketch of cell adhesion vs. water contact angle (based on literature values [6] and exemplified by our own findings) and depiction of the water contact angles on the materials investigated in the present study.

We have investigated five biomaterials with wettabilities that cover the whole spectrum; from hydrophilic (i.e., PEG-based hydrogels) via intermediate wettability, i.e., TCPS and a fluoropolymer poly(vinylidene fluoride) (PVDF) to hydrophobic materials such as PFPE and poly(dimethyl siloxane) (PDMS).

The chemical structures of the novel materials PFPE DMA and acrylate star PEG are given in Scheme 1, and the water contact angles are listed in Table 1, together with values measured for the three conventional materials TCPS, PVDF, and PDMS. It is interesting to note that some materials display contact angle hysteresis, that is, the advancing and receding contact angles differ significantly. We have determined the contact angle hysteresis for the different materials and conclude that notably the PFPE material has a significant hysteresis of 68°, as measured by the Wilhelmy plate method. On a more explanatory note, this implies that the PFPE material might reorganize its surface when under water [36], which is obviously of critical importance when studying the material in cell culture conditions (i.e., in aqueous medium).



Scheme 1

Table 1 Static and dynamic contact angles (°) and surface energies of different materials.

		PEG	TCPS	PVDF	PDMS	PFPE
Static (°)		43 ± 1.3^a	77 ± 1.5	81 ± 1.6	110 ± 1.9	110 ± 2.0
Dynamic ^b (°)	Advancing	n.d.	96 ± 1	94 ± 1	122 ± 2.4	120 ± 1.5
	Receding	n.d.	74 ± 1.8	63 ± 1.8	63 ± 3.5	52 ± 2.5
	Hysteresis	n.d.	22	32	59	68
Surface energy (mN/m)		40.1	38.8	31.0	22.4	17.3

^aCaptive bubble method.

^bWilhelmy plate method.

n.d. = not determined.

Also the hydrogel material is prone to changes when immersed in water; the water-insoluble network can take up large quantities of water and swell in the process. It is believed that this hydrated state makes hydrogels especially repellent to proteins [37–40]. Since the water contact angle could not be measured easily on this material because of the high wettability and the swelling that occurs upon contact with water, we performed contact angle measurements according to the captive bubble method, see Table 1. The value of ~43° corresponds to values reported in literature for coatings based on similar star PEG polymers [41].

Finally it should be noted that on topographically structured surfaces, the water contact angle (as measured in air) is higher than on smooth surfaces of the same material, due to the so-called Lotus effect. This effect was also observed by us.

Cell adhesion on the biomaterials

Our cell culture experiments show the following trend. As expected, the cells (fibroblasts) adhere to TCPS very shortly (within half an hour) after seeding and they spread, grow, and proliferate in a matter of (up to 24) hours (Fig. 2b). On PVDF, the cells also adhere and spread, but in a very different time frame. The flattening and spreading of the cells becomes visible only after a day (~19–22 h), see Fig. 2c (image taken after 2 days). On the two novel biomaterials (i.e., the PEG-based hydrogel and the PFPE elastomer), the cells that are visible on the surfaces are not adhered and do not spread, not even after 5 days (the images in Figs. 2a and 2d, respectively are taken after 2 days). Cell viability tests were performed and indicated that the two novel biomaterials were not cytotoxic (which was also expected based on literature results) [42–44]. Thus, it was observed that the two novel biomaterials do not support cell adhesion and growth, and this is tentatively attributed to the wettability properties, that is, the PEG material is too hydrophilic and the PFPE material is too hydrophobic for successful cell adhesion.

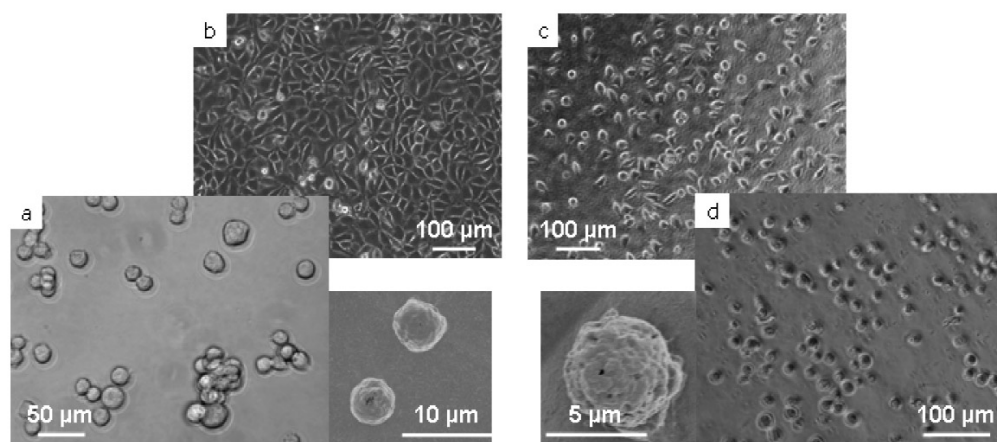


Fig. 2 Optical micrographs of cells cultured on different biomaterials; (a) PEG, (b) TCPS, (c) PVDF, (d) PFPE. Insets to (a) and (d) are scanning electron micrographs.

It is important to note that cell adhesion is not a stand-alone phenomenon and we must take into account that the cell adhesion process is preceded by protein adsorption. It has been speculated in the literature that the initially adsorbed proteins may be exchanged for others with time, and this aspect might be of unrecognized importance. The wettability of a surface is a good indicator of which proteins are preferentially adsorbed, i.e., those useful or not for cell adhesion, e.g., fibronectin or albumin, respectively [45–47]. The hydrophobicity or -philicity also determines whether the proteins will adsorb in their native conformation or are prone to undergo conformational changes. Nevertheless, with time the initially bound proteins may be exchanged by other proteins [1], unless, of course, the initially adsorbed protein (e.g., albumin) is irreversibly bound [48]. The hypothesis that in response to the biomaterial, the cell produces extracellular matrix (ECM) proteins [49] that are useful for binding and that possibly exchange the less useful proteins on the surface is very interesting, and we are currently investigating this question by means of various, time-dependent, antibody-staining experiments.

Effects of topography on cell adhesion

As extensively described in literature, cells respond strongly to topographic cues. We have investigated the two novel, UV-curable biomaterials and fabricated micro- and nanosized topographic patterns onto the surfaces, by means of UV-based nano-imprint lithography. It turned out that the cells respond in a

very pronounced manner to the microsized topographic patterns. Whereas the cells did not adhere and did not spread at all on the smooth surfaces of PEG and PFPE, on surface-structured samples the cells do adhere and adopt distinctive morphologies (Fig. 3).

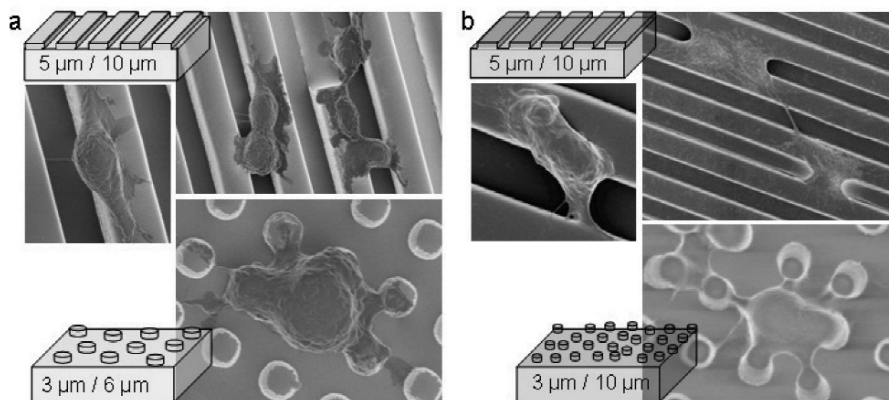


Fig. 3 Cell cultures on the novel biomaterials bearing micrometer-sized topographic patterns; (a) PEG and (b) PFPE.

In short, on micrometer grooves, the cells tend to align along the ridges as was expected based on literature reports concerning contact guidance. On micrometer posts, the cells either adhere to the sides of the posts when they are bigger than the cellular dimensions or they grab a manifold (typically 4–6) of posts on which they kind of “float” [50]. The adhesion and spreading of the cells on the structured surfaces indicate that either the amount and/or orientation of the (initial) protein adsorption is different on the topographically structured samples than on the smooth ones [51], which in the case of the hydrogel could be attributed to an increase in hydrophobicity [52,53] or that the cells respond to the topographic features themselves [54,55]. In the latter case, it was reasoned that the flexibility of cell’s cytoskeleton depends on the rigidity of (bundles of) F-actin and their adaptation to the surface’s topography determines the alignment of the cells [10]. We are currently investigating the cellular responses, at different time intervals, on topographic patterns with different geometries.

Influence of mechanical properties on cellular responses

Finally, we have started to investigate the effect of the substrate’s elasticity on the cellular behavior. Our preliminary results revealed that on topographic patterns with identical geometry of the features (i.e., 5 μm lines spaced 5 μm) but with a different elasticity of the PEG material (elastic modulus $E \sim 0.15$ or 2.6 MPa, respectively), cells either sat in the grooves or aligned along the tops of the ridges, respectively (details will be published elsewhere). In the latter case, namely, on stiffer PEG hydrogels (Fig. 3a), the behavior of the cells is comparable to that on the PFPE material (Fig. 3b), which is also relatively stiff ($E \sim 4$ MPa). We intend to vary the cross-linking density of the PFPE material as well in order to make further comparisons between the two materials and to elucidate if the substrate’s stiffness is really such an important parameter.

CONCLUSIONS

The two novel, UV-curable, and biocompatible polymers (i.e., a star-shaped PEG and a linear PFPE) are interesting biomaterials, since three characteristics of the material, namely, the chemistry, topography, and elasticity, can be varied independently. It has been demonstrated that the smooth, unstruc-

tured materials do not support cell adhesion (let alone spreading and growth), and this was tentatively attributed to the wettability; the PEG material is too hydrophilic and the PFPE elastomer is too hydrophobic. A drastic effect, however, was observed when the material was shaped against a mold during the UV-curing (cross-linking) of the prepolymers to result in a defined surface topography. On both materials, micrometer-sized surface structures elicited strong cellular responses: the cells adhered and changed their shape depending on the geometry of the features. Typically, the cells elongated along the rims of a line pattern, while they “floated” on top of a surface with pillars. It should be noted that the chemistry of the substrate is not altered by the imprinting process; smooth and topographically structured surfaces possess the same chemistry.

ACKNOWLEDGMENTS

The authors wish to thank the Alexander von Humboldt Foundation and the Federal Ministry for Education and Res. (BMBF) for funding in the form of a Sofja Kovalevskaja Award (ML).

REFERENCES

1. R. A. Latour. In *Encyclopedia of Biomaterials and Biomedical Engineering*, G. L. Bowlin, G. Wnek, (Eds.), Dekker Encyclopedias, New York (2005).
2. U. Hersel, C. Dahmen, H. Kessler. *Biomaterials* **24**, 4385 (2003).
3. J. M. Anderson. *Ann. Rev. Mater. Res.* **31**, 81 (2001).
4. G. M. Whitesides, E. Ostuni, S. Takayama, X. Y. Jiang, D. E. Ingber. *Ann. Rev. Biomed. Eng.* **3**, 335 (2001).
5. Y. Ikada. *Biomaterials* **15**, 725 (1994).
6. Y. Tamada, Y. Ikada. *J. Biomed. Mater. Res.* **28**, 783 (1994).
7. M. M. Stevens, J. H. George. *Science* **310**, 1135 (2005).
8. A. Curtis, C. Wilkinson. *Biomaterials* **18**, 1573 (1997).
9. M. J. Dalby, M. O. Riehle, H. J. H. Johnstone, S. Affrossman, A. S. G. Curtis. *Tiss. Eng.* **8**, 1099 (2002).
10. P. Uttayarat, G. K. Toworfe, F. Dietrich, P. I. Lelkes, R. J. Composto. *J. Biomed. Mater. Res. A* **75**, 668 (2005).
11. S. Jungbauer, R. Kemkemer, H. Gruler, D. Kaufmann, J. P. Spatz. *ChemPhysChem* **5**, 85 (2004).
12. A. I. Teixeira, G. A. Abrams, C. J. Murphy, P. F. Nealey. *J. Vac. Sci. Technol. B* **21**, 683 (2003).
13. R. G. Flemming, C. J. Murphy, G. A. Abrams, S. L. Goodman, P. F. Nealey. *Biomaterials* **20**, 573 (1999).
14. G. A. Dunn, A. F. Brown. *J. Cell Sci.* **83**, 313 (1986).
15. G. A. Dunn, J. P. Heath. *Exp. Cell Res.* **101**, 1 (1976).
16. P. T. Ohara, R. C. Buck. *Exp. Cell Res.* **121**, 235 (1979).
17. D. M. Brunette. *Exp. Cell Res.* **164**, 11 (1986).
18. R. Singhvi, G. Stephanopoulos, D. I. C. Wang. *Biotechnol. Bioeng.* **43**, 764 (1994).
19. D. E. Discher, P. Janmey, Y. L. Wang. *Science* **310**, 1139 (2005).
20. A. J. Engler, M. Berry, H. L. Sweeney, D. E. Discher. *Mol. Biol. Cell* **15**, 298A (2004).
21. T. Yeung, P. C. Georges, L. A. Flanagan, B. Marg, M. Ortiz, M. Funaki, N. Zahir, W. Y. Ming, V. Weaver, P. A. Janmey. *Cell Motility Cytoskeleton* **60**, 24 (2005).
22. R. J. Pelham, Y. L. Wang. *Proc. Natl. Acad. Sci. USA* **95**, 12070 (1998).
23. C. M. Lo, H. B. Wang, M. Dembo, Y. L. Wang. *Biophys. J.* **79**, 144 (2000).
24. J. Y. Wong, A. Velasco, P. Rajagopalan, Q. Pham. *Langmuir* **19**, 1908 (2003).
25. F. Brandl, F. Sommer, A. Goepferich. *Biomaterials* **28**, 134 (2007).
26. S. Britland, H. Morgan, B. Wojciak-Stodart, M. Riehle, A. Curtis, C. Wilkinson. *Exp. Cell Res.* **228**, 313 (1996).

27. A. Magnani, A. Priamo, D. Pasqui, R. Barbucci. *Mater. Sci. Eng., C* **23**, 315 (2003).
28. J. L. Charest, M. T. Eliason, A. J. García, W. P. King. *Biomaterials* **27**, 2487 (2006).
29. X. Q. Brown, K. Ookawa, J. Y. Wong. *Biomaterials* **26**, 3123 (2005).
30. P. M. Pfister, M. Wendlandt, P. Neuenschwander, U. W. Suter. *Biomaterials* **28**, 567 (2007).
31. M. C. Lensen, P. Mela, A. Mourran, J. Groll, J. Heuts, H. T. Rong, M. Moeller. *Langmuir* **23**, 7841 (2007).
32. S. R. Peyton, C. B. Raub, V. P. Keschrums, A. J. Putnam. *Biomaterials* **27**, 4881 (2006).
33. K. L. Prime, G. M. Whitesides. *J. Am. Chem. Soc.* **115**, 10714 (1993).
34. E. Ostuni, R. G. Chapman, R. E. Holmlin, S. Takayama, G. M. Whitesides. *Langmuir* **17**, 5605 (2001).
35. E. Ostuni, B. A. Grzybowski, M. Mrksich, C. S. Roberts, G. M. Whitesides. *Langmuir* **19**, 1861 (2003).
36. A. Vaidya, M. K. Chaudhury. *J. Colloid Interface Sci.* **249**, 235 (2002).
37. E. Monchaux, P. Vermette. *Langmuir* **23**, 3290 (2007).
38. E. Osterberg, K. Bergstrom, K. Holmberg, T. P. Schuman, J. A. Riggs, N. L. Burns, J. M. Vanalstine, J. M. Harris. *J. Biomed. Mater. Res.* **29**, 741 (1995).
39. P. Harder, M. Grunze, R. Dahint, G. M. Whitesides, P. E. Laibinis. *J. Phys. Chem. B* **102**, 426 (1998).
40. R. L. C. Wang, H. J. Kreuzer, M. Grunze. *J. Phys. Chem. B* **101**, 9767 (1997).
41. J. Groll, Z. Ademovic, T. Ameringer, D. Klee, M. Moeller. *Biomacromolecules* **6**, 956 (2005).
42. J. H. Harris. *Poly(ethylene glycol) Chemistry: Biotechnical and Biomedical Applications*, Plenum Press, New York (1993).
43. R. Z. Xie, M. D. M. Evans, B. Bojarski, T. C. Hughes, G. Y. Chan, X. Nguyen, J. S. Wilkie, K. M. McLean, A. Vannas, D. F. Sweeney. *Inv. Opth. Vis. Sci.* **47**, 574 (2006).
44. G. Johnson, G. F. Meijs, B. G. Laycock, M. G. Griffith, H. Chaouk, J. G. Steele. *J. Biomater. Sci.-Pol. Ed.* **10**, 217 (1999).
45. M. Lampin, R. Warocquier-Clerout, C. Legris, M. Degrange, M. F. Sigot-Luizard. *J. Biomed. Mater. Res.* **36**, 99 (1997).
46. G. K. Toworfe, R. J. Composto, C. S. Adams, I. M. Shapiro, P. Ducheyne. *J. Biomed. Mater. Res. A* **71**, 449 (2004).
47. K. Kottke-Marchant, A. A. Veenstra, R. E. Marchant. *J. Biomed. Mater. Res.* **30**, 209 (1996).
48. D. L. Elbert, J. A. Hubbell. *Ann. Rev. Mater. Sci.* **26**, 365 (1996).
49. B. K. Mann, A. T. Tsai, T. Scott-Burden, J. L. West. *Biomaterials* **20**, 2281 (1999).
50. A. M. P. Turner, N. Dowell, S. W. P. Turner, L. Kam, M. Isaacson, J. N. Turner, H. G. Craighead, W. Shain. *J. Biomed. Mater. Res.* **51**, 430 (2000).
51. E. T. den Braber, J. E. de Ruijter, L. A. Ginsel, A. F. von Recum, J. A. Jansen. *J. Biomed. Mater. Res.* **40**, 291 (1998).
52. P. Kim, D. H. Kim, B. Kim, S. K. Choi, S. H. Lee, A. Khademhosseini, R. Langer, K. Y. Suh. *Nanotechnology* **16**, 2420 (2005).
53. K. Y. Suh, S. Jon. *Langmuir* **21**, 6836 (2005).
54. T. G. van Kooten, A. F. von Recum. *Tiss. Eng.* **5**, 223 (1999).
55. L. S. Chou, J. D. Firth, V. J. Uitto, D. M. Brunette. *J. Cell Sci.* **108**, 1563 (1995).